Available online at www.sciencedirect.com
ScienceDirect
*Mendeleev Commun.*, 2012, **22**, 111–113
Mendeleev Communications

# Electrochemical reduction and radical anions of benzo[*b*]thioxanthene-6,11,12-trione and thioxanthene-1,4,9-trione

**Nadezhda V. Vasilieva, Irina G. Irtegova, Vladimir A. Loskutov and Leonid A. Shundrin***

*N. N. Vorozhtsov Novosibirsk Institute of Organic Chemistry, Siberian Branch of the Russian Academy of Sciences, 630090 Novosibirsk, Russian Federation. Fax: +7 383 330 9752; e-mail: shundrin@nioch.nsc.ru*

DOI: 10.1016/j.mencom.2012.03.021

The electrochemical reduction of benzo[*b*]thioxanthene-6,11,12-trione and thioxanthene-1,4,9-trione in DMSO, MeCN and HMPA is an EE process, which is characterized by two separate one electron reversible peaks on cyclic voltammograms, first peak retains reversibility in DMSO–$H_2O$ mixtures, corresponding radical anions were obtained by one electron reduction of the above compounds and characterized by EPR and DFT calculations at the (U)B3LYP/6-31+G* level of theory.

Thioxanthene derivatives are of interest as the photoinitiators of polymerization[1] and possess biological activity.[2] Benzo[*b*]-thioxanthene-6,11,12-trione **1** and thioxanthene-1,4,9-trione **2** (Scheme 1) reveal *in vivo* antimicrobial and anticancer activities against P-388 mouse lymphocytic leukemia.[2] Both compounds have a π-electron subsystem of the quinoid type and possess sufficiently high electron affinity (EA)[3] to undergo reversible electron transfer in liquids. Therefore, knowledge of their redox properties is important for better understanding the behaviour of **1**, **2** in living systems. On the other hand, compounds **1**, **2** can be considered as promising basic structures for the design of redox-active labels for biosensor technologies, like anthraquinone derivatives.[4]

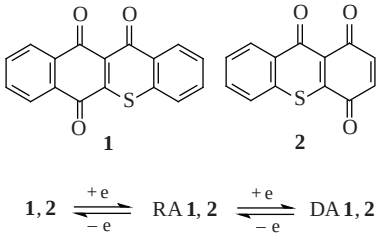


**Scheme 1**

The cyclic voltammograms (CVs)† of **1**, **2** were measured in the potential sweep region $-2.3 < E < 0.5$ V (*vs.* s.c.e.) for aprotic solvents and $-1.25$ ($-0.7$) $< E < 0.25$ V for DMSO–$H_2O$ mixtures depending on $H_2O$ content.† In aprotic solvents, CVs of both compounds revealed two reduction one electron and diffusion

† Compounds **1**, **2** were prepared as described previously.[3] Solvents for CV measurements were purified by the following methods: MeCN was twice distilled over $P_2O_5$, DMSO and HMPA were twice distilled in vacuum from $CaH_2$. The treatment of HMPA requires special care because of its carcinogenicity! All solvents were stored over 4 Å molecular sieves. The water content was < 0.5% in dry solvents. The CV measurements of **1**, **2** were performed at 298 K in an argon atmosphere in dry aprotic solvents (DMSO, MeCN and HMPA) and DMSO–$H_2O$ mixtures of various compositions at a stationary platinum electrode ($S$ = 0.08 cm$^2$) with 0.1 M $Et_4NClO_4$ as a supporting electrolyte with sweep rates of $0.1 < \nu < 1.3$ V s$^{-1}$. The PG 310 USB potentiostat (HEKA Elektronik, Germany) was used for CV measurements. Peak potentials are quoted with reference to a saturated calomel electrode (s.c.e). For **1**, **2** both reduction peaks are diffusion controlled, *i.e.*, $I_p^C \nu^{-0.5}$ = const, where $I_p^C$ is the peak current, and $\nu$ is potential sweep rate. For high concentrations of $H_2O$, potential sweep was reduced to $-0.7 < E < 0.25$ V.

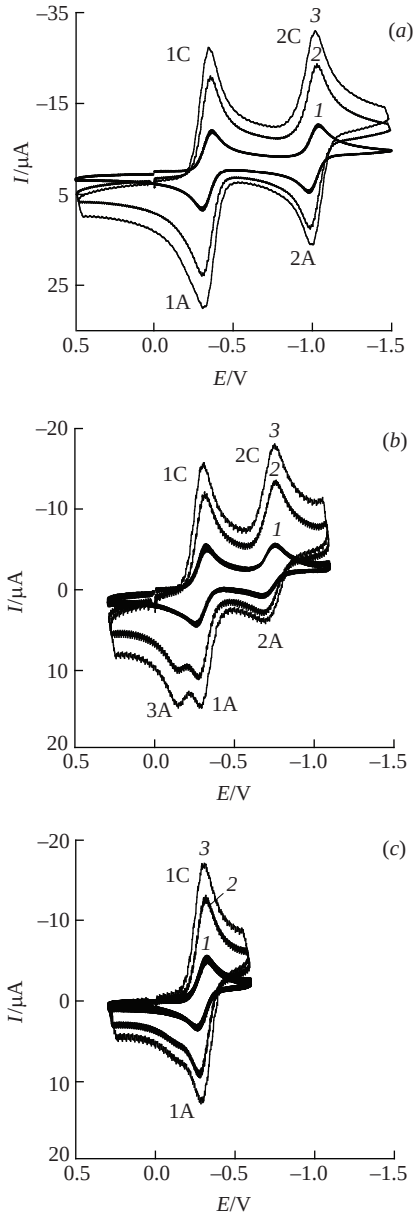


**Figure 1** CV of **1** in (*a*) DMSO and (*b*) DMSO–$H_2O$ ($m$ = 0.545) and (*c*) CV of the first peak within potential sweep $-0.7 < E < 0.25$ V in DMSO–$H_2O$ ($m$ = 0.545). (*1*) $\nu$ = 0.1, (*2*) 0.7 and (*3*) 1.3 V s$^{-1}$.

© 2012 Mendeleev Communications. All rights reserved.

**Table 1** Experimental reduction potentials of compounds **1**, **2** in aprotic solvents,[a] $H_2O$,[b] and calculated (B3LYP/6-31G*) vertical electron affinities.[c]

| Compound | Solvent | $E_p^{1C}$/V | $E_p^{1A}$/V | $E_p^{2C}$/V | $E_p^{2A}$/V | EA/eV |
|---|---|---|---|---|---|---|
| **1** | DMSO | –0.37 | –0.31 | –1.04 | –0.97 | 1.67 |
| | MeCN | –0.48 | –0.42 | –1.10 | –0.94 | |
| | HMPA | –0.34 | –0.28 | –1.18 | –1.11 | |
| | $H_2O$ | –0.22 | –0.16 | — | — | |
| **2** | DMSO | –0.22 | –0.16 | –0.90 | –0.83 | 1.76 |
| | MeCN | –0.31 | –0.24 | –1.02 | –0.94 | |
| | HMPA | –0.20 | –0.14 | –1.11 | –1.05 | |
| | $H_2O$ | 0.04 | 0.10 | — | — | |

[a] Potential sweep rate is 0.1 V $s^{-1}$. [b] First peak potentials calculated from regression (1). [c] From ref. 3.

controlled† reversible peaks corresponding to the formation of the radical anion (RA) and dianion (DA), respectively [EE process, Figure 1(*a*), example for **1** in DMSO]. Corresponding peak potentials are listed in Table 1 as $E_p^{iC}$ and $E_p^{iA}$, where *i* is the peak number in the CV curve (Figure 1), symbols C or A indicate the cathodic or anodic branch of the CV curve, respectively. The absolute values of $E_p^{1C}$ are minimal in HMPA for **1**, **2** and maximal in MeCN. The values of $E_p^{1C}$ measured in the same aprotic solvents are less negative for **2** as compared with **1**. It is in agreement with the bigger vertical EA for **2**[3] (Table 1).

The electrochemical reduction of both of the tested compounds is similar; therefore, we illustrate CV for **1** only, as an example. The second peak becomes quasi-reversible in DMSO–$H_2O$ mixtures, and the additional peak (3A) appears at the anodic branch of CV in the potential range $-0.06 < E_p^{3A} < -0.12$ V (*vs.* s.c.e) depending on potential sweep rate† [Figure 1(*b*), example for **1**]. The first peak retains reversibility in the entire range of DMSO–$H_2O$ compositions for both compounds, when potential sweep covers the first CV wave only [Figure 1(*c*)]. No additional peaks are observed in this case. The anodic peak 3A can be attributed to the oxidation of a dianion decay product.

The dependences of $E_p^{1C}$ on the molar fraction of $H_2O$ (*m*) in DMSO–$H_2O$ ($0.0 < m < 0.82$) are well described by square-law regression:

$$E_p^{1C}(m) = Am^2 + Bm + C. \quad (1)$$

The parameters *A*, *B*, *C* and *r* are 0.0622, 0.1062, –0.376, 0.995 for **1** and 0.1739, 0.1015, –0.223, 0.997 for **2**, respectively, where *r* is correlation coefficient of regressions (1). $E_p^{1C}$ for **1**, **2** in $H_2O$ were determined by the extrapolation of function (1) to $m = 1$ (Table 1).

The RAs of **1**, **2** were obtained by the one electron reduction of neutral precursors with potassium in HMPA and by electrochemical reduction in DMSO.‡ The high resolution EPR spectra‡ of the RAs of **1**, **2** in HMPA are shown in Figure 2, and the hyperfine coupling constants (HFCC) are listed in Table 2. An additional EPR signal without hyperfine structure from unknown paramagnetic species is observed in the spectrum of RA **2** [Figure 2(*b*)], but its intensity does not exceed 8% on a total intensity basis, and it does not affect the interpretation of RA **2** EPR spectrum.

‡ The EPR spectra were recorded on a Bruker ELEXSYS E540 spectrometer (MW power of 20 mW, modulation frequency of 100 KHz and modulation amplitude of 0.005 mT). The method of RA generation with potassium in HMPA is well known.[5] Both radical anions are long lived under these conditions, no decrease in total intensity of EPR signal was found during 1 h. RA of **1**, **2** were obtained also by electrochemical reduction in absolute DMSO under argon atmosphere at 298 K. In this case, the largest HFCCs are well resolved (Table 2). Simulations of the experimental EPR spectra were performed with the Winsim 2002 program[6] (the accuracy in calculating *a* is ±0.0001 mT). An arrow in Figure 2(*b*) indicates paramagnetic signal without hyperfine structure of unknown nature (~8% of total intensity).

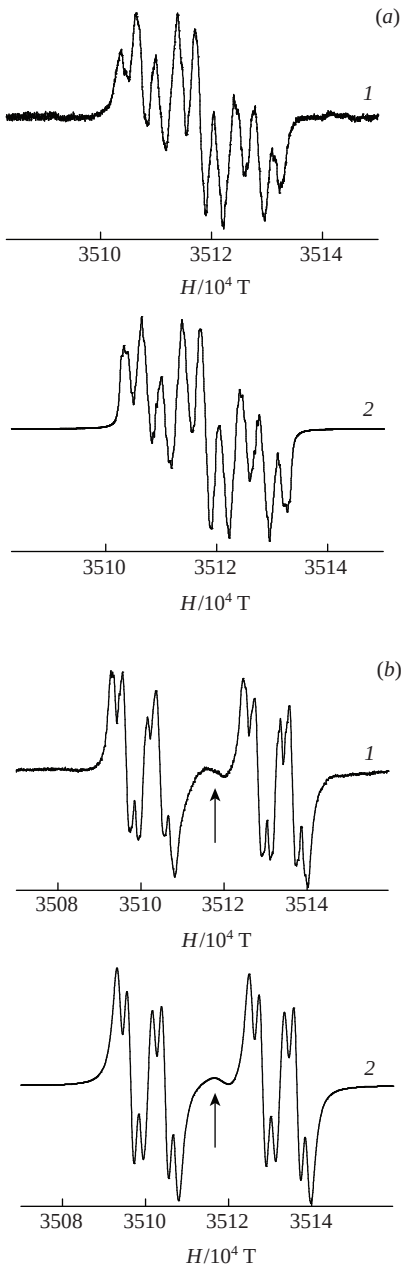


**Figure 2** EPR spectra of (*a*) RA **1** and (*b*) RA **2** at 295 K in HMPA under reduction with potassium.‡ (*1*) experiment and (*2*) simulation.

**Table 2** Experimental HFCC (mT) of the radical anions of **1**, **2** together with those calculated at the DFT/(U)B3LYP/6-31+G* level of theory.[§]

| Anion | Experimental | | (U)B3LYP/6-31+G* |
|---|---|---|---|
| | HMPA‡ | DMSO[a] | |
| **1** | 0.005 (H1) | | –0.001 (H1) |
| | 0.011 (H2) | 0.011 (H2) | –0.018 (H2) |
| | 0.009 (H3) | | 0.005 (H3) |
| | 0.030 (H4) | 0.032 (H4) | –0.026 (H4) |
| | 0.073 (H7) | 0.079 (H7) | –0.077 (H7) |
| | 0.020 (H8) | 0.020 (H8) | 0.018 (H8) |
| | 0.109 (H9) | 0.107 (H9) | –0.113 (H9) |
| | 0.038 (H10) | 0.036 (H10) | 0.051 (H10) |
| **2** | 0.318 (H2) | 0.320 (H2) | –0.343 (H2) |
| | 0.083 (H3) | 0.083 (H3) | –0.055 (H3) |
| | 0.028 (H5) | | –0.027 (H5) |
| | 0.005 (H6) | | 0.011 (H6) |
| | 0.021 (H7) | | –0.026 (H7) |
| | 0.002 (H8) | | 0.005 (H8) |

[a] Electrochemical reduction. Resolved HFCC are shown only.

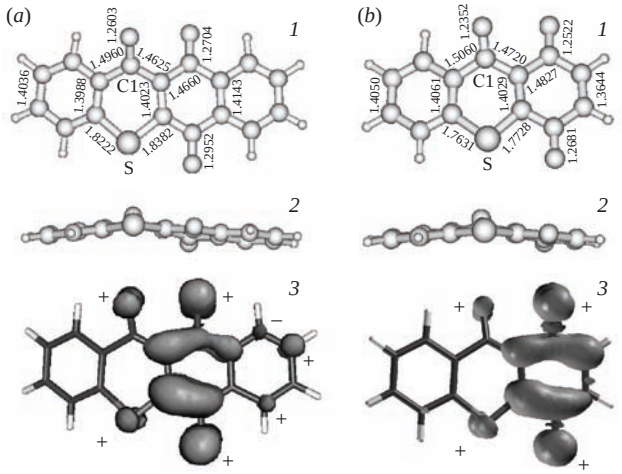


**Figure 3** (*1*) (U)B3LYP/6-31+G* geometry (bond lengths/Å), (*2*) view along C1-S bond and (*3*) single occupied molecular orbital[§] in (*a*) RA **1** and (*b*) RA **2**.

The (U)B3LYP/6-31+G* calculations[§] demonstrate that both RA are non-planar in optimized conformations, and their single occupied molecular orbital (SOMO) is of the pseudo-π type (Figure 3). In accordance with the calculations, SOMOs of both RAs are similar and localized at quinoid molecular subgraph, sulfur atom and CO group for the most part. Spin density distributions in RAs **1** and **2** indicate that two largest HFCC are related to protons in the 9,7-positions for RA **1** and the 2,3-positions for RA **2** (Table 2).

Thus, the electrochemical reduction of compounds **1**, **2** is an EE process in the test aprotic solvents and an EEC process in DMSO–$H_2O$ mixtures. The first stage of electrochemical reduction retains reversibility in the entire range of DMSO–$H_2O$ compositions. The radical anions of **1**, **2** are long lived in aprotic solvents; their geometry is nonplanar in the ground state according to (U)B3LYP/6-31+G* calculations, and SOMO is of the pseudo-π type.

This work was supported by the Russian Foundation for Basic Research (project no. 10-03-00844a).

## References

1 X. Jiang and J. Yin, *Macromol. Rapid Commun.*, 2004, **25**, 748.
2 V. K. Tandon, R. V. Singh and D. B. Yadav, *Bioorg. Med. Chem. Lett.*, 2004, **14**, 2901.
3 V. A. Loskutov and I. V. Beregovaya, *Zh. Org. Khim.*, 2009, **45**, 1418 (*Russ. J. Org. Chem.*, 2009, **45**, 1405).
4 D. A. Di Giusto, W. A. Wlassoff, S. Giesebrecht, J. J. Gooding and G. C. King, *J. Am. Chem. Soc.*, 2004, **126**, 4120.
5 M. M. Urberg and E. T. Kaiser, *J. Am. Chem. Soc.*, 1967, **89**, 5179.
6 D. R. Duling, *J. Magn. Reson.*, 1994, **104**, 105.
7 M. W. Schmidt, K. K. Baldridge, J. A. Boatz, S. T. Elbert, M. S. Gordon, J. H. Jensen, S. Koseki, N. Matsunaga, K. A. Nguyen, S. J. Su, T. L. Windus, M. Dupuis and J. A. Montgomery, *J. Comput. Chem.*, 1993, **14**, 1347.

[§] The quantum-chemical calculations were performed using the GAMESS suite of programs.[7] The geometries of RA **1**, **2** were fully optimized at the (U)B3LYP/6-31+G* level of theory for gas phase. The symbols + and – (Figure 3) indicate the signs of spin density.

*Received: 11th August 2011; Com. 11/3780*